Journal of Cluster Science, Vol. 17, No. 4, December 2006 (© 2006)
DOI: 10.1007/s10876-006-0076-7

Quantitative Non-Covalent Functionalization of Carbon Nanotubes

Anson Ma,[1] Jun Lu,[1] Shihe Yang,[2,3] and Ka Ming Ng[1]

Received July 26, 2006; published online October 10, 2006

We report a convenient method for quantitative non-covalent functionalization of single-walled carbon nanotubes (SWNT) with phthalocyanine (Pc) compounds, in which a surface coverage of 49% was achieved. The effect of several process parameters on the functionalization process was elucidated. Firstly, as-produced SWNT gave the largest extent of functionalization compared with purified SWNT and as-produced multi-walled carbon nanotubes (MWNT). Secondly, the extent of functionalization was sensitive to the specific molecular structures of the Pc compounds. Finally, in terms of solvent selection, dimethylformamide (DMF) was found to give the largest extent of functionalization, which is then followed by chloroform ($CHCl_3$) and 1,2-dichlorobenzene (ODCB). The method reported in this paper provides new insights on the interactions between Pc molecules and carbon nanotubes and paves the way for rational control of the degree of functionalization, which is an important step from the perspective of carbon nanotube applications.

KEY WORDS: Non-covalent functionalization; Phthalocyanine (Pc); carbon nanotubes.

INTRODUCTION

Since their discovery in 1991 [1], single-walled carbon nanotubes (SWNT) have received continuous interest [2] in wide-ranging fields, on account of their anisotropic shapes (diameters of around 1 nm and lengths of micrometers), remarkable strength and elasticity, high thermal and electrical

[1]Department of Chemical Engineering, The Hong Kong University of Science and Technology, Clear Water Bay, Hong Kong.
[2]Department of Chemistry, The Hong Kong University of Science and Technology, Clear Water Bay, Hong Kong.
[3]To whom correspondence should be addressed. E-mail: chsyang@ust.hk

conductivities. To fully exploit the promising properties of carbon nanotubes, numerous attempts have been carried out to functionalize carbon nanotubes [3–7]. Functionalization can further be classified as covalent or non-covalent, depending on the type of intermolecular interaction involved. In general, non-covalent functionalization is more preferable as this type of functionalization can preserve the wall integrity and thus intrinsic electronic properties of carbon nanotubes [8–10]. Non-covalent functionalization normally involves molecules with planar moieties that could adsorb onto the surfaces of carbon nanotubes via $\pi - \pi$ interactions. For instance, functionalization of SWNT with porphyrin was reported by Chen and Collier [11]. Wang *et al.* [8] showed that phthalocyanines (Pc) can be bound non-covalently to multi-walled carbon nanotubes, and the composite was found to have promising application as the electrode of a glucose sensor [12].

With ongoing efforts in developing new types of non-covalently functionalized carbon nanotube materials and exploring their specific applications, it is of paramount importance to understand the $\pi - \pi$ interactions in more details and develop strategies to control the functionalization. To our knowledge, however, systematic studies towards this direction have been lacking thus far [8–12]. Herein, we report a convenient method for quantitative non-covalent functionalization of carbon nanotubes with phthalocyanine (Pc) compounds. A surface coverage of 49% was achieved for purified SWNT. With this method, we have also investigated several key parameters of the functionalization process, including the types of carbon nanotubes, Pc compounds, and solvents used.

EXPERIMENTAL

Materials

Single-wall carbon nanotubes used in this study ($d \sim 1.2$ nm) were as-produced grade (a-SWNT) sourced from Carbon Solutions Inc. They were produced by the arc-discharge method and were purified using a two-step oxidation method [13–16]. 1 g of as-produced SWNT was first oxidized in air at 300°C for 30 min, and then refluxed in 300 mL nitric acid (3 M) for 5 h. Purified single-walled nanotubes were referred as p-SWNT herein after. Multi-wall carbon nanotubes (MWNT, $d \sim 20$ nm) were as-produced grade sourced from Helix Material Solutions, Inc. They were produced by the chemical vapor deposition method. Two different types of Pc compounds were used in this study: 2, 9, 16, 23-Tetra-tert-butyl-29H,31H-phthalocya-

nine (TBPc) and Copper(II), 9, 16, 23-tetra-tert-butyl-29H,31H-phthalocyanine (CuTBPc). Both of them were purchased from Aldrich. Solvents used include dimethylformamide (DMF) (Bayer, HPLC grade), chloroform ($CHCl_3$) (BDH, AR-grade), and 1, 2-dichlorobenzene (ODCB) (Aldrich, Reagent-grade). All of the chemicals were used without further purification.

Functionalization Protocol

In a typical run, 5 mg of single-walled nanotube sample (a-SWNT/p-SWNT) was weighed into a 20 ml solution of Pc (50 μg/mL-DMF). The mixture was then sonicated for 1 h. A cup-horn type sonicator equipped with a water cooling system from Branson Ultrasonics Corporation was used for the sonication because it allows for both power and temperature control. Power intensity was kept at 40 W for all experimental runs. The functionalization was carried out at room temperature. Room temperature was maintained by the water cooling system in the sonication cup.

Characterization

Pc-functionalized SWNT was characterized by Infra-Red (IR) spectroscopy (Perkin Elmer, Spectrum One), UV-Vis spectroscopy (Perkin Elmer, Lambda 20), and Transmission Electron Microscopy (TEM) (JEOL, TEM 2010). Samples used for IR spectroscopy were prepared by first mixing/grinding the carbon nanotubes with potassium bromide (KBr) and then pressing the mixtures into pellet forms. Specific surface area of p-SWNT was measured by nitrogen-BET method and the analyzer used was COULTER^{TM} SA 3100. The samples were degassed at 250°C for 2 h prior to the analysis.

Quantification Protocol

The extent of Pc functionalization was determined by measuring the amount of Pc rendered in the solution phase at a particular time. A stop watch was used to keep track of time and the moment that sonication started was referenced as time = 0. During sonication, 1.5 mL of the solution was withdrawn using a glass syringe at different time intervals. Solid in the solution was filtrated and the absorbance of the solution was measured after 10 times dilution. In order to correlate the absorbance with the Pc concentration in the solution, calibration curves (see Supporting Information for example) were produced by measuring the absorbance of Pc

solution at different concentration levels (1, 2, 5, 7.5, 10 μg/mL). Finally, the amount of Pc functionalized was calculated by subtracting the amount of Pc rendered in the solution from the initial amount.

RESULTS AND DISCUSSION

Functionalization of SWNT with CuTBPc

Although the ultrathin layer of CuTBPc could not be discerned by TEM (see Supporting Information S-I), successful functionalization of SWNT with CuTBPc was substantiated by IR and UV-Vis spectroscopy. Figure 1 shows IR spectra of SWNT, CuTBPc, and their complex. CuTBPc shows two characteristic peaks at 2866 and 2956 cm^{-1}, which are due to C–H stretching modes in the tert-butyl group. The complex resembles these peaks at 2856 and 2925 cm^{-1}, respectively, as shown in the inset picture of Fig. 1. Besides, a red-shift of the C=C stretching mode of the carbon nanotubes is also observed from 1600 cm^{-1} for p-SWNT to 1584 cm^{-1} for the complex. Redshifts in the wave-numbers of characteristic peaks can be explained by electron delocalization due to $\pi - \pi$ interactions [8]. In other words, non-covalent anchoring of Pc onto SWNT was achieved via $\pi - \pi$ stacking [7].

UV–Vis spectra of SWNT, CuTBPc, and their complex were obtained by re-dispersing solid sample in DMF. As shown in Fig. 2A, SWNT shows

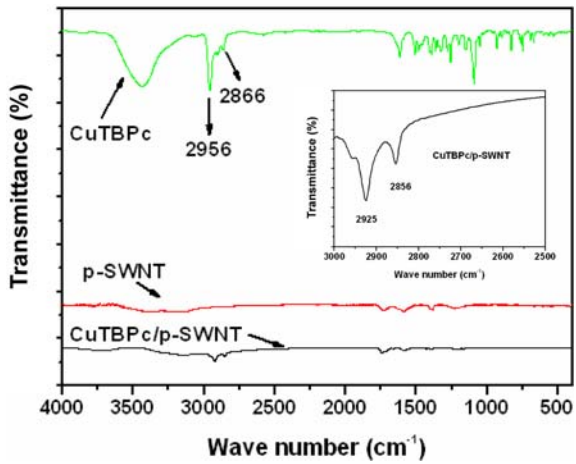

Fig. 1. IR Spectra (KBr Pellet) of SWNT, CuTBPc, and their complex.

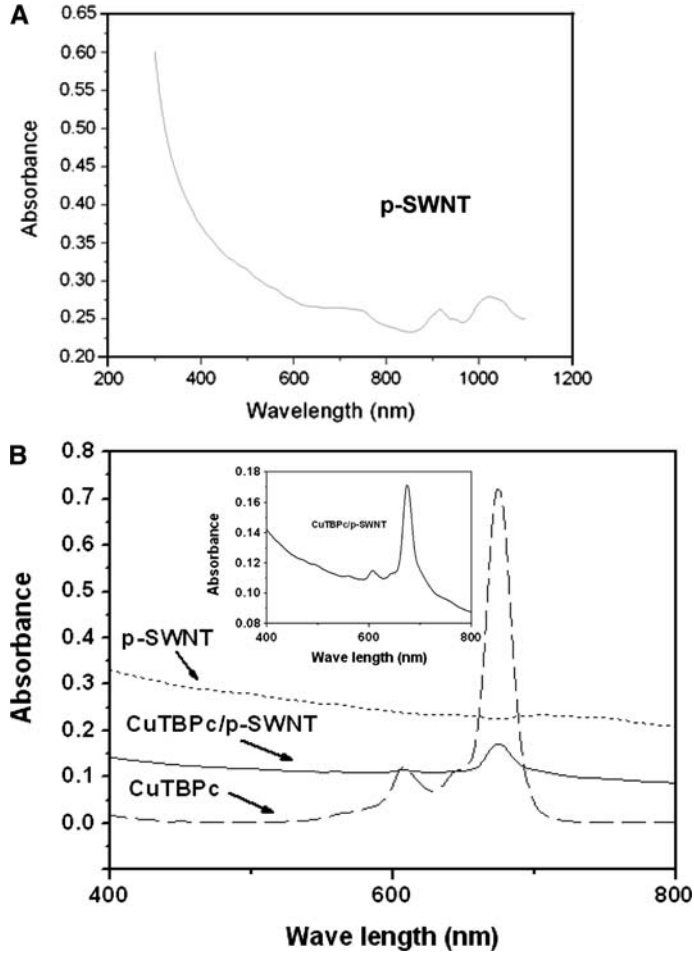

Fig. 2. (A) UV–Vis spectrum of SWNT; (B) UV-Vis spectra of SWNT, CuTBPc, and their Complex.

characteristic peaks at 740 nm (M_{11}), 910 nm (S_{22}), and 1300 nm (S_{11}). M_{11} is known as the singularity transition for metallic nanotubes, whilst S_{11} and S_{22} are singularity transitions for semiconducting nanotubes [17, 18]. For CuTBPc, characteristic peaks were observed at 608 nm and 674 nm (Fig. 2B), whilst the complex sample resembles these peaks as shown in the inset picture.

Extent of Functionalization

By measuring the amount of Pc rendered in solution, the amount of Pc functionalized can be calculated by simple mass balance (see Supporting Information S-II). The extent of functionalization as a function of time can then be plotted, as shown in Fig. 3. However, this method relies on one crucial assumption that Pc does not decompose within the time frame of interest. As a result, control tests in which Pc solutions are sonicated in the absence of nanotube were carried out to validate the assumption. Detailed results of the control tests are included in the Supporting Information S-III.

The amount of CuTBPc functionalized on SWNT was calculated to be 0.046 [g-Pc/g-SWNT]. The N_2 adsorption isotherm (77 K) of the p-SWNT is of Type IV in IUPAC classification, having a hysteresis loop. The isotherm is shown in the Supporting Information S-IV. This is in agreement with the work of Yang *et al.* [19]. From BET studies, the surface area of p-SWNT was found to be 258.04 m^2/g (0.0051 nm^2/carbon atom). This value is smaller than the value obtained by assuming that all carbon nanotubes are de-bundled, which gives a value of 0.026 nm^2/carbon atom. Above all, based on the surface area estimated by BET, about 49% of the surface was covered by CuTBPc (See Supporting Information S-V).

Effect of Nanotube Type

Figure 4 shows the functionalization curves of three different types of carbon nanotubes. They are as-produced single-walled carbon nanotubes (a-SWNT), purified single-walled carbon nanotubes (p-SWNT), and

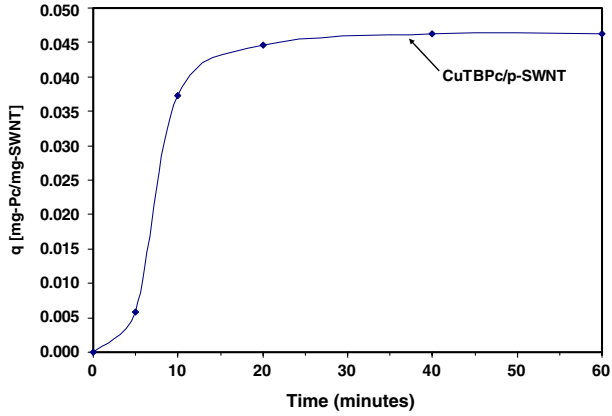

Fig. 3. Functionalization curve of the base-case (p-SWNT/CuTBPc/DMF).

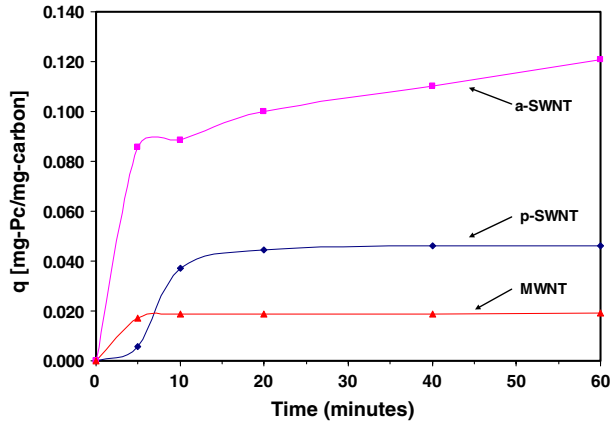

Fig. 4. Functionalization curves of p-SWNT, a-SWNT, and MWNT.

as-produced multi-walled carbon nanotubes (MWNT). Compared with p-SWNT, a-SWNT possesses a higher capacity for CuTBPc immobilization. This can be attributed to relatively small amount of functional group moieties on the walls of a-SWNT, which perturb $\pi - \pi$ interactions between SWNT and CuTBPc. Because a-SWNT has not gone through the purification process, the amount of functional group moieties on the walls of a-SWNT should be less than that of p-SWNT. For MWNT, the extent of functionalization is the smallest. This can be explained by the fact that only the outer surface of MWNT is accessible to CuTBPc. Therefore, despite the fact that some of the SWNT exist in small bundles, the total surface area per unit mass of MWNT is smaller than that of SWNT. A remark is in order as to whether the inner walls of the CNTs could be adsorption sites of the Pc-type molecules. Because the mean diameter of the SWNTs used in this work is $\sim$1.2 nm, it seems unlikely for a Pc-derivative molecule to absorb into the inner tube of SWNT. Although the MWNTs we used have a inner diameter range of $\sim$4–8 nm, the ends of the MWNTs are closed. Even though defects may exist, it still seems difficult for the Pc-derived molecule to go into the inner tubes of the MWNTs.

Effect of Pc Type

Functionalization of two different types of Pc was investigated in this study. CuTBPc and TBPc have almost the same peripheral structure. The only difference lies in the central part. CuTBPc has a metal ion in the central

cavity, whilst TBPc does not (Fig. 5). Figure 5 shows functionalization curves of p-SWNT with CuTBPc and TBPc. The extent of functionalization for CuTBPc is less than that for TBPc. This can be explained by the presence of coordination bonds between copper and nitrogen, which hinders effective $\pi - \pi$ interactions between SWNT and CuTBPc. Similar phenomenon has been reported for MWNTs [8]. However, our study is the first one to provide a quantitative account on the difference between the non-coordinated and metal-coordinated Pcs and thus offer a more quantitative and precise way to compare the two in terms of their aptitude to functionalize CNTs.

Effect of Solvent

Figure 6 shows functionalization curves of p-SWNT with CuTBPc obtained by using three different solvents, namely DMF, $CHCl_3$, and ODCB. The amount of CuTBPc functionalized is the largest when DMF was used as the solvent. This can be attributed to the debundling effect of DMF [20, 21], which has increased the total surface area for functionalization to take place. On the other hand, although ODCB was also reported to be capable of dispersing nanotubes [22], the amount of CuTBPc functionalized is the smallest when it was used as the solvent. This can possibly be explained by considering the type of interaction between Pc and nanotube. $\pi - \pi$ interactions were primarily responsible for the binding process of Pc onto the walls of SWNT. However, ODCB also possesses a benzene ring that interacts with nanotubes via the same mechanism. Besides that, it was also reported that under sonication, certain amount of ODCB would polymerize and wrap around SWNT [23]. Therefore, relatively low

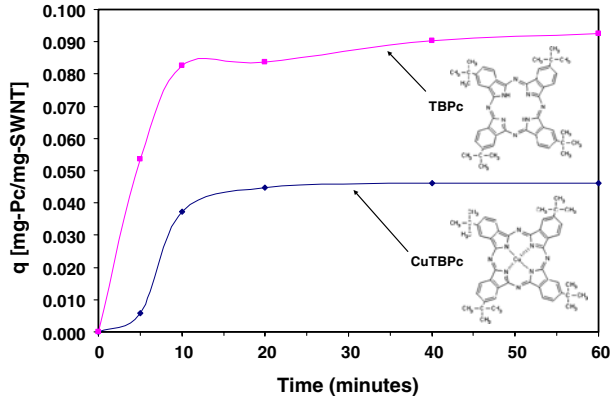

Fig. 5. Functionalization of p-SWNT with CuTBPc and TBPc.

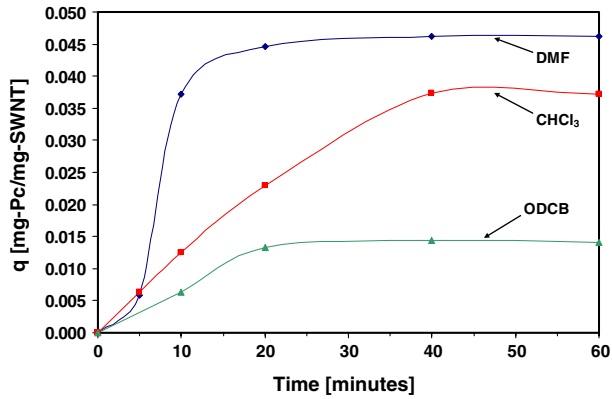

Fig. 6. Functionalization of p-SWNT with CuTBPc in different solvents.

extent of functionalization in ODCB is very likely to be a result of competition between the solvent – ODCB, and the solute – CuTBPc [24].

CONCLUSIONS

In short, quantitative non-covalent functionalization of SWNT with Pc was reported and a surface coverage of 49% was achieved. The method reported has been successfully applied to provide new insights on the interactions between SWNT and Pc. It has been found quantitatively that the types of carbon nanotubes, Pc compounds, and solvents all played important roles in the functionalization process. The largest extent of functionalization can be achieved for as-produced SWNT, TBPc, and DMF respectively. Apart from the functionalization of SWNT with Pc compounds, it is envisaged that the same technique can serve as a useful tool for other types of non-covalent functionalization. By doing so, more in-depth thermodynamic as well as kinetic studies of different types of non-covalent functionalization can be carried out. In essence, this technique has laid the foundation for rational control of end products' functionality, which is important from the perspective of product development and nanotube applications.

ELECTRONIC SUPPLEMENTARY MATERIAL

Supplementary material for this article is avilable at http://www.dx.doi.org/10.1007/s10876-006-0076-7 and is accessible for authorised users.

ACKNOWLEDGMENT

This project is supported by ITC069/02.

REFERENCES

1. S. Iijima (1991). *Nature (London)* **354**, 56.
2. P. M. Ajayan (1999). *Chem. Rev.* **99**, 1787.
3. S. S. Wong, E. Joselevich, A. T. Woolley, C. L. Cheung, and C. M. Lieber (1998). *Nature* **394**, 52.
4. K. Kamaras, M. E. Itkis, H. Hu, B. Zhao, and R. C. Haddon (2003). *Science* **301**, 1501.
5. A. Hirsch (2002). *Angewandte Chemie International Edition* **41**(11), 1853.
6. V. Georgakilas, K. Kordatos, M. Prato, D. M. Guldi, M. Holzinger, and A. J. Hirsch (2002). *J. Am. Chem. Soc.* **124**(5), 760.
7. D. Tasis, N. Tagmatarchis, V. Georgakilas, and M. Prato (2003). *Chem. Eur. J.* **9**, 4000.
8. X. Wang, Y. Liu, W. Qiu, and D. Zhu (2002). *J. Mat. Chem.* **12**, 1636.
9. H. Murakami, T. Nomura, and N. Nakashima (2003). *Chem. Phys. Lett.* **378**, 481.
10. R. J. Chen, Y. G. Zhan, D. W. Wang, and H. J. Dai (2001). *J. Am. Chem. Soc.* **123**(16), 3838.
11. J. Chen and C. P. Collier (2005). *J. Phys. Chem. B* **109**, 7605.
12. J.-S. Ye, Y. Wen, W. D. Zhang, H. F. Cui, G. Q. Xu, and F.-S. Sheu (2005). *Electroanalysis* **17**(1), 89.
13. C. A. Furtado, U. J. Kim, H. R. Gutierrez, L. Pan, E. C. Dickey, and P. C. Eklund (2004). *J. Am. Chem. Soc.* **126**, 6095.
14. S. Bandow, A. M. Rao, K. A. Williams, A. Thess, R. E. Smalley, and P. C. Eklund (1997). *J. Phys. Chem. B,* **101**, 8839.
15. J. M. Moon, K. H. An, and Y. H. Lee (2001). *J. Phys. Chem. B* **105**, 5677.
16. B. Zheng, Y. Li, and J. Liu (2002). *Appl. Phys. A* **74**, 345–348.
17. S. Banerjee and S. S. Wong (2002). *J. Phys. Chem. B* **106**, 12144.
18. Z. Chen, X. Du, M. H. Du, C. D. Rancken, H. P. Cheng, and A. G. Rinzler (2003). *Nano Lett.* **3**(9), 1245.
19. C. M. Yang, K. Kaneko, M. Yudasaka, and S. Iijima (2002). *Physica B* **323**, 140.
20. K. D. Ausman, R. Piner, O. Lourie, R. S. Ruoff, and M. Korobov (2000). *J. Phys. Chem.* B, **104**(38), 8911.
21. C. A. Furtado, U. J. Kim, H. R. Gutierrez, L. Pan, E. C. Dickey, and P. C. Eklund (2004). *J. Am. Chem. Soc.* **126**, 6095.
22. J. L. Bahr, E. T. Mickelson, M. J. Bronikowski, R. E. Smalley, and J. M. Tour (2001). *Chem. Commun.*, 193.
23. S. Niyogi, M. A. Hamon, D. E. Perea, C. B. Kang, B. Zhao, S. K. Pal, A. E. Wyant, M. E. Itkis, and R. C. Haddon (2003). *J. Phys. Chem. B* **107**, 8799.
24. F. Rouquerol, J. Rouquerol, and K. Sing, *Adsorption by Powders and Porous Solids: Principles, Methodology and Application* (Academic Press, U.K, 1999).